

The Paddle: A novel procedure for artificial gust generation in a wind tunnel

The Paddle: Ein neuartiges Verfahren zur Erzeugung künstlicher Windböen im Windkanal

J. N. Wood and M. Breuer

Professur für Strömungsmechanik, Helmut-Schmidt-Universität / Universität der Bundeswehr Hamburg

Artificial (horizontal) wind gust, wind tunnel experiments, fluid-structure interaction
Künstliche (horizontale) Windböen, Windkanal-Experiment, Fluid-Struktur-Interaktion

Abstract

The following contribution is based on the study carried out by Wood et al. (2022) dealing with a novel wind gust generator (WGG) used to generate horizontal gusts in a wind tunnel. The presented device denoted “*The Paddle*” is composed of a rigid plate mounted onto a fast-moving tooth belt axis. The plate is used to alter the flow at the beginning of the test section by temporally blocking the outlet plane of the nozzle with a defined blocking ratio. The dynamic motion of the paddle generates an artificial gust with a well-defined shape imposed onto the free-stream flow of the wind tunnel. Laser-Doppler measurements are carried out at various positions in the test section in order to characterize the unsteady and the ensemble-averaged flow. It is shown that the shape and intensity of the generated gust is highly reproducible and can be customized based on the free parameters of the paddle motion.

Introduction

Extreme weather events such as heavy storms are expected to occur more often in the future as an effect of the climate change. Especially wind gusts are a potential threat to the public and cause severe damage to buildings and other infrastructure. Therefore, a profound understanding of the effects of wind gusts on (lightweight) structures is necessary to adapt the constructions accordingly. Unfortunately, the atmospheric effects causing the formation of wind gusts are highly complex rendering a practical implementation in wind tunnel tests rather difficult. Furthermore, measurements at real scales are challenging and often accompanied with high costs. Therefore, a feasible alternative is based on small-scale experimental investigations. This motivates the present study which focuses on the artificial generation of wind gusts at lab scale providing the opportunity to study the effect of gusts on buildings under controlled conditions. This methodology allows to investigate critical flow conditions that may lead to structural damages and failure.

For this purpose, a novel approach to generate unsteady velocity variations of short duration that are imposed on the steady free-stream of a wind tunnel is suggested (Wood et al., 2022) to mimic the effects of horizontal wind gusts. A new wind gust generator denoted “*The Paddle*” is proposed based on a rigid plate mounted on a fast-moving tooth belt axis. The device is installed at the outlet of the nozzle to alter the free-stream flow at the beginning of the test

section. The principle of the *paddle* is simple: The steady flow leaving the nozzle is altered dynamically by a fast down- and upward motion of the plate in vertical direction. This leads to a temporal blocking of a defined area of the outlet plane. The result is a sudden acceleration of the flow approximately following a 1-cosine velocity signal which is comparable to an Extreme Coherent Gust as defined by the European Aviation Safety Agency (2015). To characterize the performance of the *paddle*, a predefined motion pattern is investigated. An extensive measurement campaign based on laser-Doppler anemometer (LDA) data shows that the generated horizontal gusts are highly reproducible. Only minor variations are detected in the core area of the gust which are attributed to the free-stream turbulence of the wind tunnel. The next section presents the actual design of the *paddle* and the experimental setup with all relevant parameters.

The *Paddle* and the experimental setup

The design of the *paddle* is based on a cost-efficient retrofit solution installed into the current wind tunnel setup. All components are selected from a commercial manufacturer of electric automation tools (Festo Vertrieb GmbH & Co. KG) including the software to access all parameters of the device. A schematic representation of the *paddle* including its integration into the test section of the wind tunnel is depicted in Fig. 1.

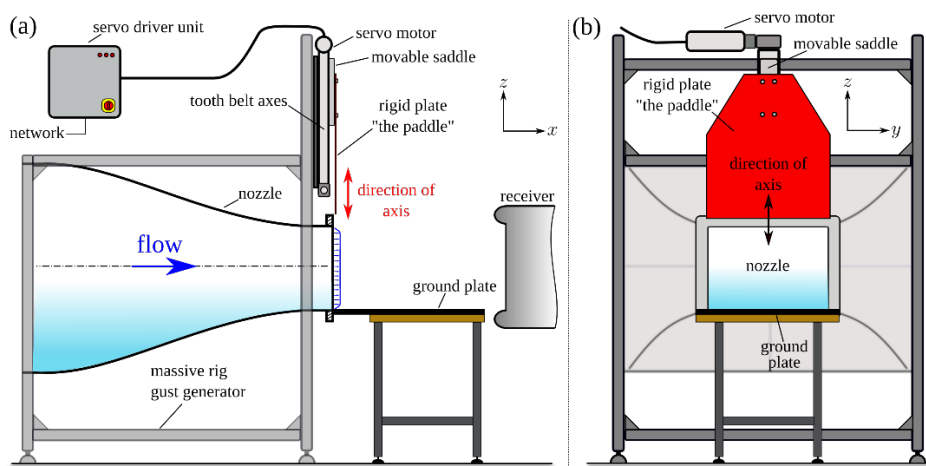


Fig. 1: Schematic of the *paddle* implemented into the wind tunnel setup (Wood et al., 2022).

The hardware of the *paddle* is composed of a tooth belt axis with a movable saddle to which a rigid aluminum plate (red) is mounted. Furthermore, it includes a servo motor and a servo driver unit. The tooth belt axis is mounted onto a rigid rig and positioned at the beginning of the test section (Fig. 1(a)) of the wind tunnel above the outlet of the nozzle. A small gap of 0.015 m is considered between the aluminum plate and the nozzle ensuring a free motion of the plate avoiding the risk of damage. The rigid plate is covering the complete spanwise dimension of the nozzle outlet plane (Fig. 1(b)). Additionally, a ground plate is aligned horizontally with the lower wall of the nozzle to transfer the flow from the nozzle to the test section. The ground plate is necessary to generate horizontal gusts which shall be later used for fluid-structure interaction experiments with flexible structures under gust loads.

The *paddle* is controlled by the software tool Festo Automation Suite granting access to all relevant kinematic parameters of the servo motor (displacement, velocity, acceleration and jerk). The actual parameters of the *paddle* and the current settings are listed in Table 1. These parameters are defined in an automated referencing process inside the software and are strongly depending on the orientation of the tooth belt axes (horizontal/vertical) and the

applied mass connected to its saddle. In the current case the tooth belt axis is positioned so that the mounted plate dives vertically into the free-stream of the wind tunnel.

Table 1: Specification and actual setup of the parameters of the *paddle*.

Feature	Value
Max. stroke length (displacement)	0.3 m
Max. possible blocking ratio of nozzle outlet	0.8
Mass of aluminum plate connected to saddle	3.24 kg
Max. velocity	± 4.74 m/s
Max. acceleration	± 27 m/s ²
Positioning accuracy	± 0.08 mm
Temperature range	-10 °C $\leq \vartheta \leq 70$ °C

To validate the performance of the *paddle*, experimental investigations are carried out in a closed-loop sub-sonic wind tunnel with an open test section with dimensions $0.8 \text{ m} \times 0.5 \text{ m} \times 0.375 \text{ m}$ ($l \times w \times h$). The ground plate ($0.6 \text{ m} \times 0.6 \text{ m}$) is placed at the bottom of the test section adjoined to the nozzle outlet (see Fig. 1(a)). A laser-Doppler anemometer (TSI PowerSight, 2D-probe) is positioned outside the free-stream flow. Details of the wind tunnel and the LDA settings including the measurement campaign can be found in Wood et al. (2022). The underlying principle of the *paddle* are discussed in detail in the next section.

Principle of gust generation

The main feature of the *paddle* is the generation of horizontal gusts imposed onto the free-stream flow. This idea is schematically sketched in Fig. 2 showing the gust generation procedure at six characteristic time steps in chronological order.

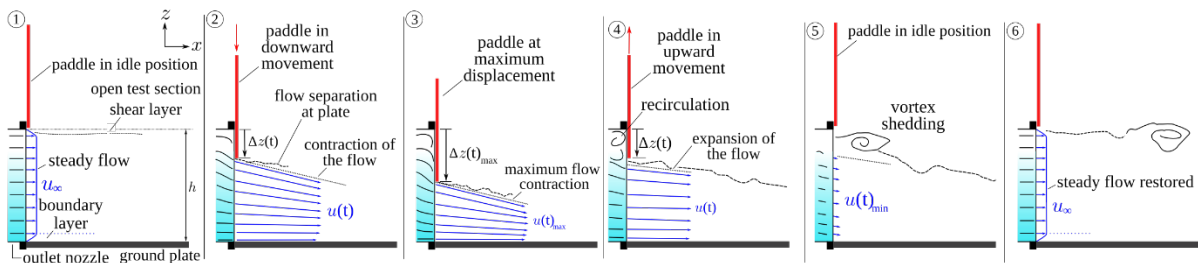


Fig. 2: Sketch of the gust generation procedure (Wood et al., 2022).

Instant ①: The wind tunnel is operating in its normal mode at the steady free-stream velocity u_∞ at the outlet of the nozzle. At the bottom wall the boundary layer continues to grow along the ground plate. The *paddle* (red) is in idle position without moving. Its lower edge is placed slightly above the upper outlet wall without disturbing the free-stream flow.

Instant ②: The *paddle* starts its vertical downward motion diving into the free-stream which leads to the displacement $\Delta z(t)$ contracting the flow. With increasing reduction of the outlet area, the flow accelerates causing the unsteady flow velocity $u(t)$. Additionally, the blocking of the plate leads to a vertical velocity component directed towards the horizontal ground plate which magnitude decreases towards the surface. A flow separation occurs at the bottom edge of the *paddle* dividing the flow into two regions: An accelerated flow field, where the artificial gust is forming, and the separated flow region above it indicated by the dashed line.

Instant ③: The *paddle* reaches the maximum displacement $\Delta z(t)_{\max}$ which is associated with the maximum flow velocity $u(t)_{\max}$. The flow contraction is further increasing in streamwise direction, thus reducing the size of the area that is unaffected by the developing shear layer (*paddle* edge) at positions further downstream.

Instant ④: The *paddle* reverses and moves upwards again leading to a flow expansion which causes the unsteady flow velocity $u(t)$ to decrease. Due to the large blocking by the *paddle*, a recirculation area develops in the nozzle in front of the *paddle*.

Instant ⑤: The *paddle* arrives at its idle position again. The recirculating flow caused by the blocking is shed as a large vortex traveling downstream with the flow. The original outlet area of the nozzle is restored. However, the low momentum flow caused by the recirculation and the increased resistance of the wind tunnel due to the *paddle* motion leads to an undershoot of the flow velocity with a minimum velocity $u(t)_{\min}$, which is lower than the undisturbed free-stream velocity u_{∞} .

Instant ⑥: After a short restitution phase the undisturbed free-stream flow is recovered.

The next section outlines the parameters of the *paddle* for a selected application case.

Parameter settings of the *paddle*

The main advantage of the *paddle* is the possibility to customize its movement allowing to define specific motion patterns for individual gust shapes. The predefined patterns can be recorded to correlate the dynamics of the *paddle* with the flow measurements of the corresponding gust. The study by Wood et al. (2022) considers five different motion patterns. To keep it brief here, only the most important pattern denoted “the standard gust shape (Type 1)” is outlined in the following. The kinematic characteristics of the Type 1 gust is depicted in Fig. 3. The parameters are set to mimic the 1-cosine gust shape considered by the IEC-Standard (2002) denoted as Extreme Coherent Gust (IEC-Standard 61400-21). This specific gust model is often used to validate the effect of gusts on the performance of wind turbines. To achieve this characteristic gust shape, the parameters of the Type 1 gust are set to perform a fast symmetric down-up movement. The motion of the *paddle* shows a bell-shaped displacement pattern which is in good agreement with the considered 1-cosine model. The displacement graph in Fig. 3 is divided by a horizontal line leading to the definition of two specific displacements denoted Δz_{OS} and Δz_{max} . The displacement Δz_{OS} denotes an offset between the lower edge of the *paddle* in idle position and the upper wall of the nozzle outlet.

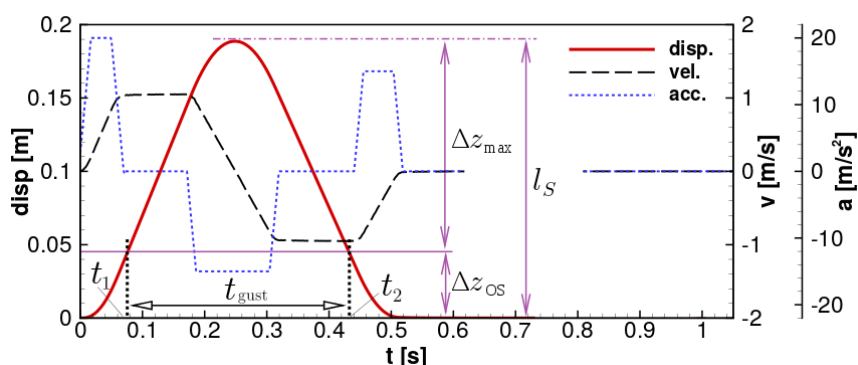


Fig. 3: Kinematic characteristics of the motion pattern “standard gust Type 1” (Wood et al., 2022).

This allows the *paddle* to achieve two effects: First, the offset avoids an interaction between the undisturbed free-stream flow and the *paddle* in idle position. Second, due to the offset the *paddle* builds up a certain velocity before diving into the free-stream flow resulting in an in-

crease of the gust amplitude. In the actual case the *paddle* enters the free-stream after passing the displacement of $\Delta z_{os} = 0.045$ m at the indicated instant in time $t_1 = 0.076$ s. Note that the zero point of the time axis is defined by the onset of the movement of the *paddle*. After exceeding the offset, the *paddle* passes into the free-stream flow leading to the predefined maximum displacement $\Delta z_{max} = 0.145$ m which is the maximum length of the *paddle* protruding into the flow. That corresponds to a blocking ratio of 0.387 which is about one half of the maximum blocking ratio possible (Table 1). When reaching the maximum displacement at 0.25 s, the *paddle* is accelerated upward again. The *paddle* leaves the free-stream flow at the time $t_2 = 0.432$ s. The elapsed time between t_1 and t_2 is denoted the gust generation time $\Delta t_{gust} = 0.356$ s. One complete stroke cycle, i.e., the time period between two idle positions of the *paddle*, is given by $\Delta t_{WGG} = 0.62$ s. This time increment includes the stroke length $l_s = \Delta z_{os} + \Delta z_{max} = 0.19$ m.

The corresponding velocity signal of two successive Type 1 gusts measured by LDA is shown in Fig. 4.

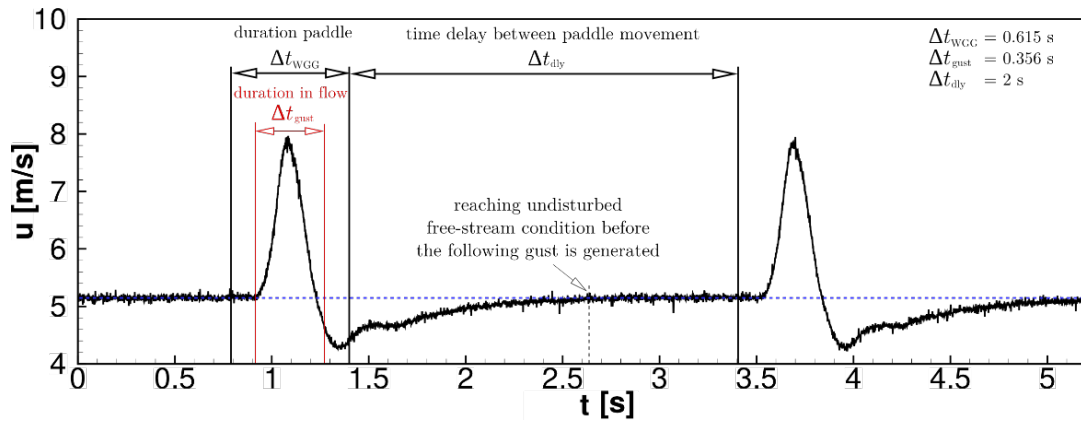


Fig. 4: Example of an LDA measurement for two successive gusts of Type 1 (Wood et al., 2022).

The wind tunnel is operating at a constant free-stream velocity $u_{\infty} = 5.14$ m/s. At about $t = 0.91$ s the *paddle* starts to dive into the flow causing a sudden increase of the velocity up to a maximum velocity of $u_{max} = 8.1$ m/s at $t = 1.09$ s. Afterwards the velocity decreases to a minimum of $u_{min} = 4.1$ m/s at $t = 1.35$ s which is lower than the free-stream velocity u_{∞} . The undisturbed free-stream velocity is recovered at about $t = 2.62$ s yielding a time interval of about $\Delta t = 1.71$ s in which the influence of the gust on the flow is detectable. After a time-delay of $\Delta t_{dly} = 2$ s counted from the time the *paddle* reaches its idle position, it is set into motion again and the wind gust generation process starts anew. The LDA signals of both gusts are in very close agreement which proves a very good reproducibility. Based on this procedure a detailed characterization of the gust is given in the next section.

Gust characteristics

The following discussion is based on a comparison between the non-dimensional unsteady and ensemble-averaged velocity signals and the corresponding fluctuations. The data focuses on the streamwise and wall-normal velocity component (u and w). The normalized quantities are based on the undisturbed free-stream velocity u_{∞} , the time t , and the length $\ell = 0.5$ m. Measurements of the gust signals are carried out at the monitoring points shown in Fig. 5. First, the detailed gust characteristics are discussed for the monitoring point located at $x/\ell = 0.2$ and $z/\ell = 0.05$. This is the location where typically a wind tunnel model for FSI investigations will be placed. Furthermore, the development of the gust along the streamwise direction is outlined based on 11 points along this direction at the height $z/\ell = 0.15$.

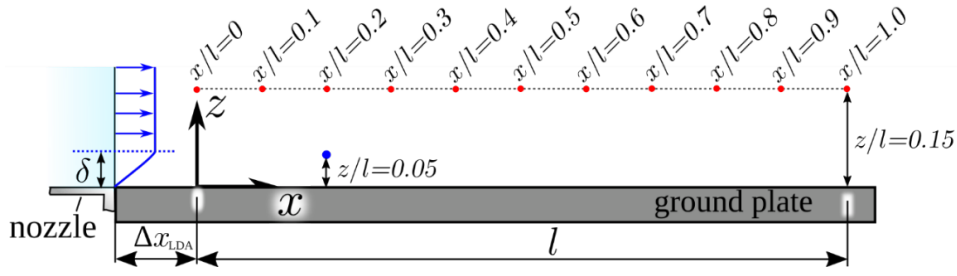


Fig. 5: Position of the monitoring points with reference to the defined coordinate system.

An offset $\Delta x_{LDA} = 0.06$ m appears between the coordinate system and the outlet plane of the nozzle due to restrictions of the LDA system. The measurements consider a sample of 25 gusts used for the ensemble averaging indicated by angular brackets. First, the comparison of the unsteady (blue) and ensemble-averaged (red) velocity signals are presented in Fig. 6.

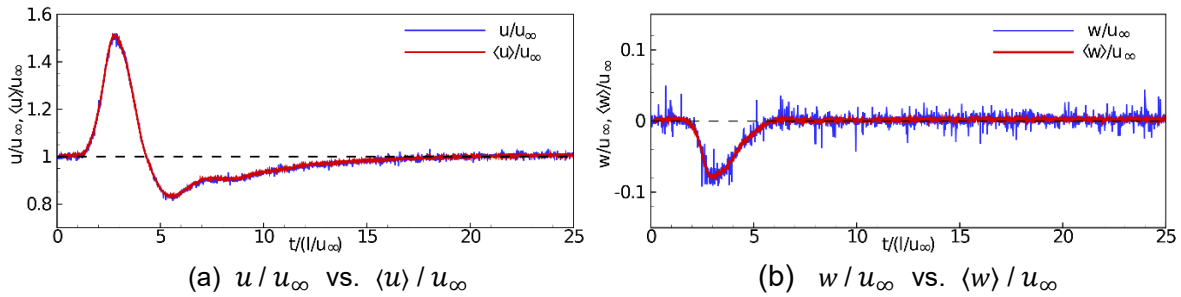


Fig. 6: Comparison of the streamwise and wall-normal velocity signals (unsteady: blue; ensemble-averaged: red) normalized by the undisturbed streamwise velocity u_∞ (Wood et al., 2022).

The streamwise velocity (Fig. 6(a)) follows the symmetry of the motion pattern of the *paddle* (Fig. 3) which is clearly reflected by the shape of the gust. The maximum gust velocity is found at $u_{\max} / u_\infty \approx \langle u_{\max} \rangle / u_\infty = 1.53$. An undershoot of the velocity results in a minimum velocity $u_{\min} / u_\infty \approx \langle u_{\min} \rangle / u_\infty = 0.88$. Moreover, the velocity fluctuations of the unsteady flow are mainly driven by the free-stream turbulence of the wind tunnel. In general, all features of the gust are fully represented by the unsteady flow. The only difference to the ensemble-averaged data is that the free-stream velocity fluctuations are averaged out resulting in a smoother time history.

The wall-normal velocity (Fig. 6(b)) shows a steeper slope on the rising flank of the gust resulting in an asymmetrical signal. The minimum wall-normal gust velocity appears at $w_{\min} / u_\infty \approx \langle w_{\min} \rangle / u_\infty = -0.08$.

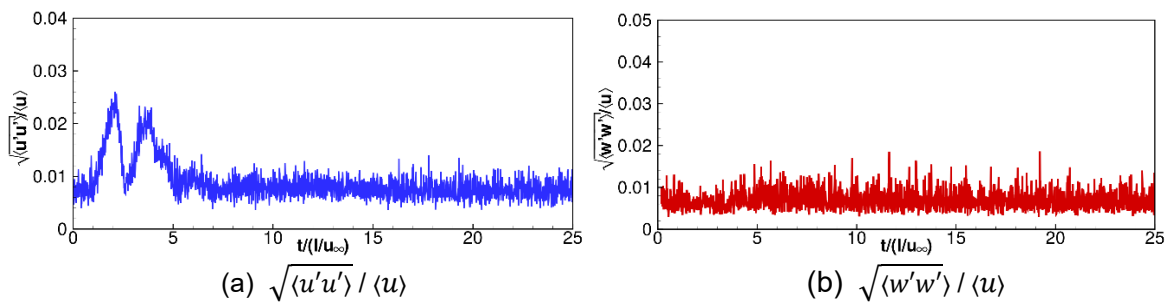


Fig. 7: Velocity fluctuations of the streamwise and wall-normal components normalized by the ensemble-averaged streamwise velocity $\langle u \rangle$ (Wood et al., 2022).

The time histories of the velocity fluctuations are depicted in Fig. 7. Both graphs correspond to the ensemble-averaged data shown in Fig. 6 and are normalized by the ensemble-averaged streamwise velocity $\langle u \rangle$. Obviously, the already mentioned free-stream turbulence of the wind tunnel in the order of about 1% or less is present. Solely during the passing of the gust with significant temporal derivatives slightly higher values up to about 2.5% are detected in case of the streamwise velocity component (Fig. 7(a)). No significant increase of the fluctuations of the wall-normal velocity can be detected in the data. Thus, the free-stream turbulence hardly influences the arising gust velocity, which is the main reason for the good reproducibility of the wind gusts. However, this only holds true for the region which is unaffected by the flow separation caused by the lower edge of the *paddle*.

The development of the Type 1 gust at the 11 positions in streamwise direction are depicted in Fig. 8.

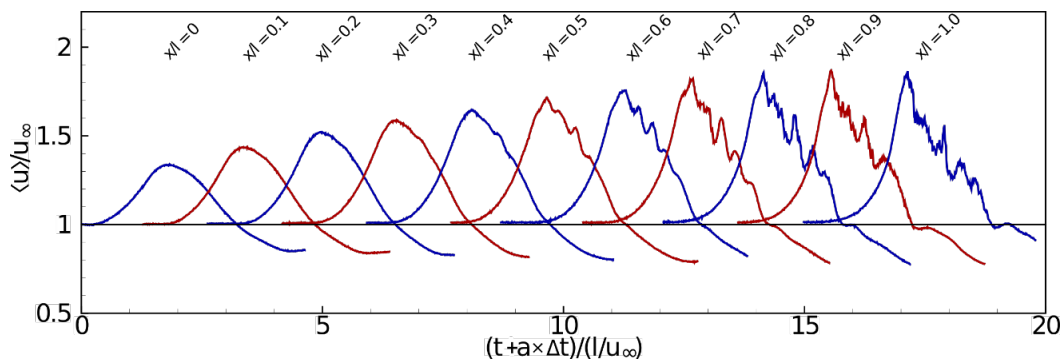


Fig. 8: Development of the ensemble-averaged streamwise velocity of the gust at various positions in streamwise direction at a given height $z/l = 0.15$ (Wood et al., 2022).

The signals are measured at a non-dimensional height $z/l = 0.15$ above the ground plate. All monitoring points are located in the symmetry plane representing a position where typically the wind tunnel model is located. Each velocity signal is shifted by a freely chosen time increment of $\Delta t = 0.15$ s multiplied with a spacing factor $a \in (0, \dots, 10)$ in order to achieve a better visualization of the data. The following main characteristics can be observed:

- The maximum gust velocity increases in streamwise direction.
- In the region ranging between $0 \leq x/l \leq 0.4$ the velocity signal of the gust is smooth and strongly correlated with the initial motion pattern of the *paddle*
- At positions $x/l \geq 0.5$ the falling slope of the gust signals exhibits an increasingly chaotic character. This is especially noticed in the time histories in the range between $0.7 \leq x/l \leq 1.0$. In contrast to the signals in the upstream part, strong velocity peaks, i.e., “velocity spikes”, arise on the falling flank. The cause for these significant fluctuations is strong turbulence observed in the shear layer that is separating at the lower edge of the *paddle* while it is moving in the free-stream.

Finally, the spanwise character of the gusts is presented in Fig. 9 showing a 3-D plot of the ensemble-averaged streamwise velocity focusing at the three streamwise locations $x/l = 0.2, 0.3$ and 0.4 at the fixed height $z/l = 0.05$. The plot shows that the gusts form in a two-dimensional manner across a range between $-0.3 \leq y/l \leq 0.3$. The remaining properties of the gust are consistent with the observations made for the symmetry plane. The increase of the gust velocity and its maximum are found to be constant in spanwise direction. The 2-D characteristic of the gust is favorable for future FSI experiments offering simple and reproducible inflow conditions.

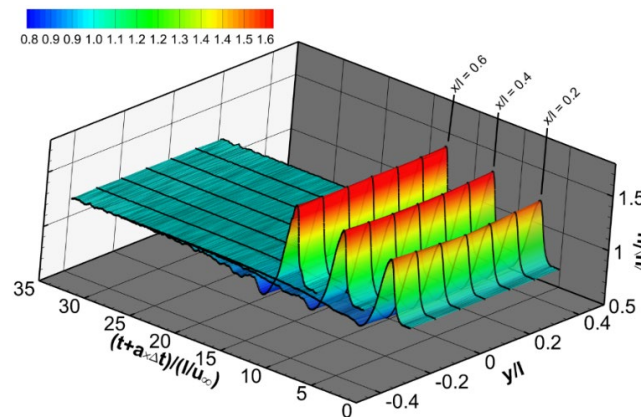


Fig. 9: Spatio-temporal development of the gust. The color bar defines the ratio of the ensemble-averaged streamwise velocity to the streamwise free-stream velocity (Wood et al., 2022).

Conclusions and outlook

A new type of wind gust generator denoted the *paddle* is presented. It is built from standard commercial components and can be retrofitted into any classic wind tunnel test section. The working principle is simple: By partially blocking the outlet of the wind tunnel nozzle with the *paddle*, the flow is strongly accelerated. Since the movement of the *paddle* can be arbitrarily defined regarding the distance covered as well as the velocity and acceleration present during the downward and upward stroke, the resulting gust can be set as desired within given limits. Streamwise and wall-normal velocity components of the generated gusts are measured by LDA in order to characterize the performance of the *paddle*. This investigation confirms a high reproducibility of the gusts within a certain region of the test section where the velocity signal is undisturbed. At the borders of the undisturbed gust area the free shear layer arising at the lower edge of the *paddle* induces strong velocity fluctuations. Consequently, the usable region for gust measurements is restricted. The size of the undisturbed area can be increased or reduced by setting the maximum displacement of the *paddle* accordingly.

As an outlook the application of the *paddle* for FSI investigations of gusts hitting flexible structures are intended for the near future. The elastic structures will orient on modern constructions that interact strongly with transient wind loads such as large-span tents consisting of flexible membranes. Combined and synchronized PIV and DIC measurements for the fluid flow and the structure deformation, respectively, are intended to be carried out soon. Moreover, a combination of the *paddle* with additionally installed turbulence generators to generate a turbulent boundary layer are considered. Furthermore, the principle of the *paddle* is currently implemented in numerical simulations to study its effects on a broader data basis. Last, the undesired effects arising from the shear layer are tackled to increase the quality of the gusts within the complete streamwise range of the test section. Therefore, a new nozzle design based on a moveable upper wall is currently in development and tested in a small-scale wind tunnel.

References

- IEC-Standard**, 2002. 61400-21. Tech. Rep., Measurement and Assessment of Power Quality of Grid Connected Wind Turbines.
- Wood, J.N., Breuer, M., Neumann, T. 2022:** "A novel approach for artificially generating horizontal wind gusts based on a movable plate: The Paddle", J. of Wind Engineering & Ind. Aerodynamics, vol. 230, 105170 (available as golden open access article).